
STRUCTURE OF MATTER
AND QUANTUM CHEMISTRY

Motion of a Lithium Ion over a Graphene–Silicene Channel: A Computer Model

O. R. Rakhmanova* and A. E. Galashev

Institute of High-Temperature Electrochemistry, Ural Branch, Russian Academy of Sciences, Yekaterinburg, 620137 Russia

**e-mail: rakhmanova@ihte.uran.ru*

Received April 29, 2016

Abstract—The motion of a lithium ion over a channel formed by sheets of perfect and defect (with monovacancies) silicene with a graphene support at different values of the channel gap is studied by means of molecular dynamics. It is established that the lithium ion enters the channel and passes through it at gap widths of 0.75 and 0.8 nm; at the same time, the monovacancies in the silicene sheets have a decelerating effect on the lithium transport over the channel. The ion passes through the channel in 12.6 and 8.6 ps for ideal silicene and 27.7 and 31.8 ps for defect silicene, respectively. It is shown that graphene sheets have a stabilizing effect that prevents the gap value from changing appreciably.

Keywords: lithium, graphene-silicene channel, monovacancies, trajectory of the motion, channel width

DOI: 10.1134/S003602441705020X

INTRODUCTION

Silicene (graphene-like silicon) is a sheet formed of single-layer silicon with a considerable effect of sp^2 -hybridization and the formation of non-planar hexagonal cells. Its unique electron properties are leading to the large-scale use of silicene in the production of high-speed electron devices. The possibility of epitaxial growth in stable silicene on Ag (111) and Ag (100) substrates in the form of narrow, virtually parallel periodic bands 2 nm high was demonstrated experimentally in [1]. Silicene is not an ideally flat object. Since sp^3 hybridization in silicon is more stable than sp^2 hybridization, the curved structure that is the average state between the two types of hybridization for silicene is energetically advantageous [2]. At room temperature, the long silicene bands have a structure with a wave-like curvature and can even intertwine in tubes when they are in the free state [3]. Two-layer silicene with AB -type packing can retain a stable 2D structure, and it is easier to obtain such a system experimentally than a monolayer sheet [4]. The cohesion energy of two-layer silicene is 5.32 eV, the interplane distance is 2.481 Å, and the curvature in this case exceeds that of single-layer silicene: 0.659 Å [4].

Introducing defects (vacancies) into two-dimensional materials via laser irradiation or with an electron beam allows us to alter their properties considerably [5]. Point defects change the local structure and reduce the thermal stability of silicene [6]. Any type of vacancy results in considerable rearrangement of the local structure of the hexagonal environment in silicene. However, its ribbed structure reduces the sys-

tem's energy and stabilizes vacancies [7]. In experiments, defect silicene is obtained much more easily than ideal silicene. This material is considered a replacement for the graphite anodes in rechargeable lithium-ion batteries. However, one of the main problems of using silicene as an anode is the considerable change in the volume of a silicon electrode during lithium transport [8]. It has been found experimentally that introducing such materials as carbon-coated silicon nanotubes [9], nanocomposites [10], and nanowires [11] into an anode can effectively suppress the change of the volume and improve the battery's capacity. Density functional calculations show that unlike crystal silicon, free two-layer silicene does not undergo considerable structural changes during the lithiation/delithiation process, and the change in its volume is no greater than 25% [12].

The aim of this work was a molecular dynamics study of the processes of lithium ion transport over silicene channels of different widths and supported by graphene sheets on both sides, and to consider the effect of defects (monovacancies) created in silicene on the structure of the system and the dynamics of lithium ion passage.

MOLECULAR DYNAMICS MODEL

Interatomic interactions in silicene (Si–Si), graphene (C–C), and between sheets of them (Si–C) were represented by the multi-particle Tersoff potential [13] with the parameters in [14]. The Tersoff potential is easily applied to bond orbitals, and param-

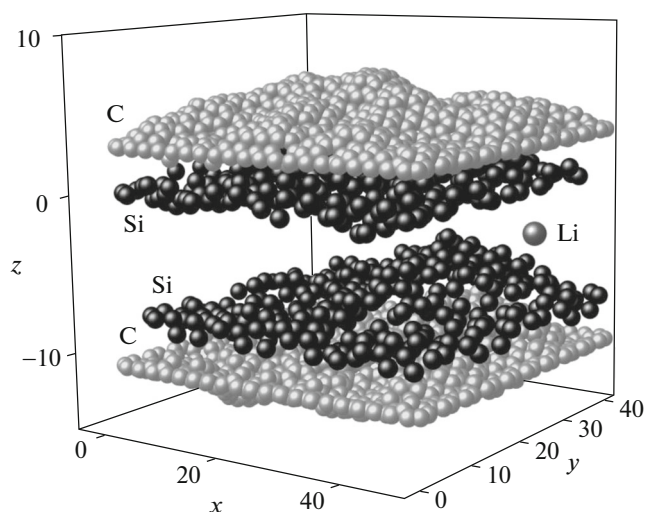


Fig. 1. Configuration of the graphene-silicene channel corresponding to the time of 9 ps, when the lithium ion leaves the channel. The gap value is 0.8 nm. Coordinates of the atoms are given in angstroms.

eters fitted to sp^3 -hybridization can be used to describe interaction in materials with sp^2 -hybridization [15]. The interaction between Si atoms belonging to different silicene sheets was described by the Morse potential [16]. The parameters of this potential were determined using interpolation relations [16–18].

This model requires the reconstruction of a 4×4 surface. The unit cell of such a silicene structure contains 18 Si atoms and has a rhombic shape. The six Si atoms of a unit cell lie perpendicular to the surface at distances of 0.074 nm, and other Si atoms are located on the same (initial) plane. The initial structure of the silicene sheet is close to the silicene surface observed on Ag(111)-substrate [19]. If the Si atoms protruding above the initial surface in the upper sheet of two-layer silicene are displaced upward, such atoms protrude downward in the lower sheet.

We first simulated a planar channel formed of two sheets of perfect (defect-free) silicene supported by graphene sheets from the outside. The lithium ion passed over a channel having different values of the gap h_g starting at 0.60 nm and ending at 0.80 nm with the step $\Delta h_g = 0.05$ nm. Our sheets of perfect silicene contained 300 atoms each and had a rectangular shape of 4.7×4.0 nm (12 Si atoms lay along each edge of the sheet). The silicene sheets were then modified with defects. Nine monovacancies were spread almost uniformly over the area of the silicene sheet, so that the number of Si atoms in each sheet was 291. A constant electric field with a strength of 10^5 V/m accelerated the Li^+ ion along the ox axis oriented over the zigzag direction of graphene sheet. The initial location of the ion corresponded to a height of $h_g/2$. At $t = 0$, the ion was at the point with coordinates $x = 0.198$ nm, $y =$

2.245 nm; i.e., it was slightly shifted into the silicene channel. Silicene sheets were arranged in accordance with Bernal packing (*ABAB...*) just as in volume graphite. Graphene sheets were placed parallel to the silicene sheets outside the channel, and the distance between the two types of sheets was the same as in [20]: 0.222 nm. The front edges of the graphene and silicene sheets forming the entry into the channel overlapped. Each rectangular graphene sheet contained 820 atoms (20 carbon atoms along each graphene edge). Boundary graphene and silicene atoms were fixed over the perimeters of the sheets; i.e., the boundary conditions corresponded to a physical experiment with a mounting frame.

The equations of motion were solved numerically using the fourth-order Runge–Kutta approach with time step $\Delta t = 1 \times 10^{-16}$ s. The duration of each calculation with gap value h_g for both perfect and defect silicene was 1×10^6 time steps, or 100 ps. Calculations were performed using the codes of the LAMMPS program complex [21]. The calculations were performed on the URAN cluster-type hybrid computer at the Institute of Mathematics and Mechanics, Ural Branch, Russian Academy of Sciences, with a peak performance of 216 Tflop/s and 1864 CPU.

RESULTS AND DISCUSSION

The first series of calculations was performed using defect-free silicene at four gaps of the graphene-silicene channel (0.6, 0.7, 0.75, and 0.8 nm). The volume configuration of the system with the gap of 0.75 nm corresponding to a time of 9 ps (the time the ion exits from the channel) is shown in Fig. 1. The passage of the lithium ion inserts a correction into the change of the shape of the graphene-silicene channel. A Li^+ ion could not enter the channel at the gap value of 0.6 nm, so the shape of the channel was not altered appreciably. The gap of 0.7 nm allowed the ion to enter, but it could not leave the channel. Considerable vertical fluctuations (up to 0.25 nm) of the atoms forming the lower silicene and graphene sheets were in this case observed. At gaps of 0.75 and 0.8 nm, the ion passes the channel correcting its sizes. The introduction of the graphene structure prevents any major changes in the volume of the system. For all considered configurations, the system returns to a configuration close to the initial one after the ion exits the channel, and any sharp changes in the shape of sheet are smoothed. However, the ruffling caused by the silicene structure can now be traced in the graphene sheets.

The passage of a Li^+ ion along the channel was also studied in calculations with monovacancies in silicene, performed at the same gap values. As with ideal silicene, the ion could not enter a channel with a gap of 0.6 nm. Neither could it enter a channel with a gap of 0.7 nm. With such gaps, the Li^+ ion made vertical fluctuating motions near the left-hand boundary of

Time a lithium ion exits graphene-silicene channel, ps

Defects in silicene	Gap value between silicene sheets, nm			
	0.6	0.7	0.75	0.8
No	Does not enter the channel	Does not exit the channel	12.6	8.6
Monovacancies	Does not enter the channel	Does not enter the channel	27.7	31.8

the channel. As in our earlier series of calculations, channel widths of 0.75 and 0.8 nm allowed comfortable transport of a Li^+ ion over a silicene channel with monovacancies. The shape and volume of the channel varied only moderately (vertical displacements of atoms were no greater than 0.12 nm). Table presents data on the time required for a Li^+ ion to pass through a graphene-silicene channel in perfect and defect silicene sheets. The presence of monovacancies in silicene creates an additional obstacle to the propagation of the ion by slowing it down. The time needed for the Li^+ ion to pass through the channel is in this case 2–3 times longer than with the defect-free silicene structure.

A schematic of the trajectory of the motion of a Li^+ ion through the channel is shown in Fig. 2 for (a) ideal silicene and (b) silicene filled with monovacancies. The gap value is 0.75 nm. Points 1 and 2 correspond to the places where the Li^+ ion enters the channel and exits from it. When the silicene sheets forming the channel are perfect, the transport of the ion under the action of a field moving horizontally occurs almost rectilinearly, and the Li^+ ion easily passes through the channel (Fig. 2a). With monovacancies in the silicene, the trajectory of the ion in the channel is crooked, and the Li^+ tends to exit the channel through vacancies (Fig. 2b).

During our MD calculations, we found there is an energy barrier at the entrance to the channel. It was shown in ab initio calculations [8] that an energy barrier of 0.88 eV must be overcome for a lithium ion to penetrate the thin silicon film on the (100) surface from its valley to the internal tetrahedral cavity. The energy for further propagation of the ion (near-surface transport) is 0.50 eV. The energy barrier for the propagation of the lithium in two-layer silicene in the free state was estimated as 0.6 eV using the density functional theory [12]. According to our MD calculations, lithium ions with energies of 0.5–2 eV can easily enter the graphene-silicene channel (and propagate in it) when the channel gap more than 0.75 nm. These MD calculations also indicate there is a barrier to the ion's exiting the channel. The determining factors are in this case not only the initial ion energy and gap value but also the channel's configuration. As a result of the tendency of silicene to create a rippled surface, the exit from the channel could be narrowed, preventing the Li^+ from exiting the channel.

Figure 3 shows xy projections of the upper (a) and lower (b) silicene sheets when the gap value was 0.6 nm. Projections correspond to a time of 100 ps, and the sheets in this case initially contained nine monovacancies each. Since the lithium ion did not enter the graphene-silicene channel in this system either, we were able to trace the life of defects without regard for the ion. In the upper sheet, three monovacancies were transformed into two five-member rings over time, one was transformed into a nine-member

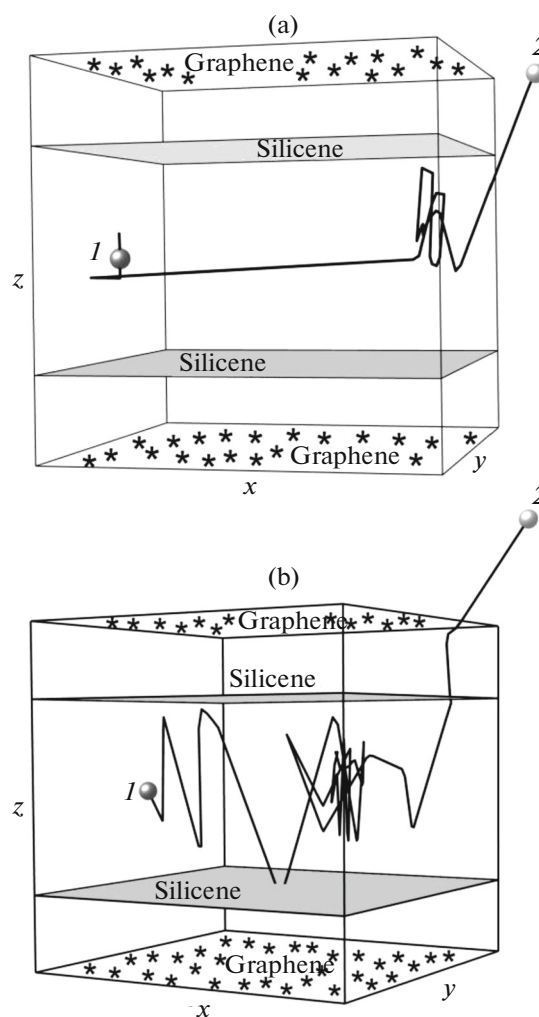


Fig. 2. Trajectory of the motion of a Li^+ ion in the graphene-silicene channel: (a) defect-free silicene, (b) silicene sheets filled with monovacancies. The gap value is 0.75 nm.

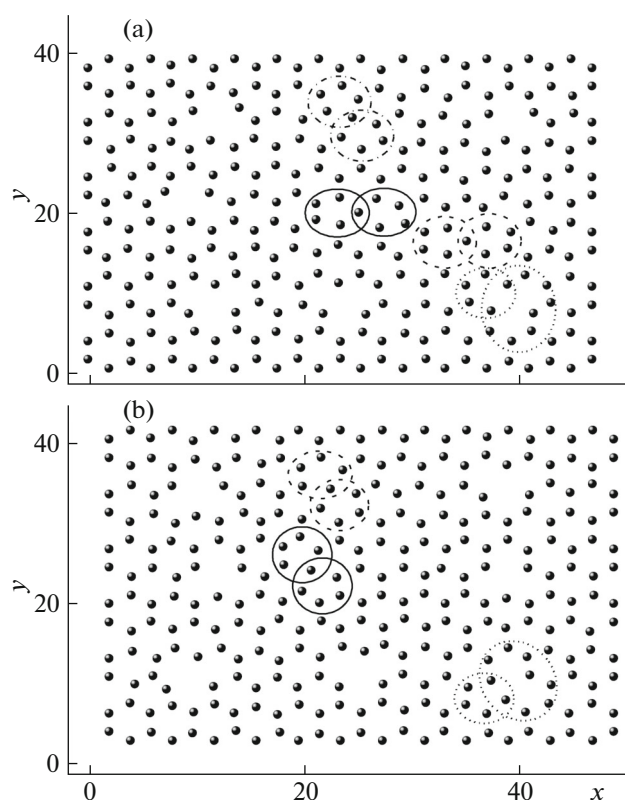


Fig. 3. *xy* projections of the (a) upper and (b) lower silicene sheets containing monovacancies, obtained at times up to 100 ps. The gap value is 0.6 nm. Transformed monodefects are denoted by ovals.

ring, and one was transformed into a five-member ring. Similar changes for three of nine point defects were observed in the lower sheet. This behavior of the monovacancies is in agreement with the density functional theory calculations when a monovacancy formed by the removal of one Si atom is transformed into two five-member rings or in one five- and one nine-member ring with one broken bond [6]. Each monovacancy prior to relaxation has three broken bonds. Being metastable structures, monovacancies can be reconstructed to reduce the number of broken bonds in the system. When an even number of atoms is eliminated in a two-dimensional structure, all broken bonds are saturated after relaxation; when an odd number of atoms is eliminated, broken bonds can be left behind [6]. The energy of the formation of monovacancies in silicene upon the removal of one Si atom is estimated to be 2.610 eV [7]. The scenario of the coalescence of several small defects into one large defect is also possible. The energy of the formation of two monovacancies (5.220 eV) is much greater than that of one bivacancy (3.217 eV), assuming that one bivacancy in silicene is a more energetically advantageous structure than two monovacancies [7]. MD ab initio calculations at a temperature of 500 K show that two neighboring monovacancies in silicene can

combine and transform into a bivacancy structure in 2 ps [7]. In our calculations, the transformation of one monovacancy into two five-member rings occurs in 3–4 ps. The formation of bivacancies was not observed in this work, since all monodefects in our systems were non-neighboring. When the gap value was 0.75 and 0.8 nm (and a lithium ion passed through the channel), we also observed the transformation of monovacancies into five-member rings in both silicene sheets. When this happened, only two or three defects evolved, while the others remained unchanged.

CONCLUSIONS

The passage of a lithium ion along a graphene-silicene channel formed by sheets of perfect and defect silicene at different gap values was considered by means of classical molecular dynamics. With defect-free silicene, the Li^+ ion could not enter the channel when it was 0.6 nm wide, or exit the channel if the gap was 0.7 nm. When the channel walls formed by silicene were modified with monovacancies, the ion could not enter at these gap values. At gap values of 0.75 and 0.8 nm, the ion passed through the channel in 12.6 and 8.6 ps (ideal silicene) and 27.7 and 31.8 ps (defect silicene), respectively. No appreciable changes in the shape or volume of the graphene-silicene channel were observed. In our calculations, the monovacancies in silicene sheets had a tendency to transform into a system of two five-member rings or one five- and one nine-member ring.

The low energy barrier to the propagation of lithium over silicene and the considerable resistance of silicene to the processes of lithiation/delithiation form a good basis for creating lithium-ion batteries with higher energy densities and longer lifetimes.

ACKNOWLEDGMENTS

This work was supported by the Russian Science Foundation, project no. 16-13-00061; and by RF Government Regulation no. 211, contract no. 02.A03.21.0006.

REFERENCES

1. G. L. Lay, B. Aufray, C. Leandri, et al., *Appl. Surf. Sci.* **256**, 524 (2009).
2. S. Cahangirov, M. Topsakal, E. Akturk, et al., *Phys. Rev. Lett.* **102**, 236804 (2009).
3. A. Ince and S. Erkos, *Comp. Mater. Sci.* **50**, 865 (2011).
4. W. Rui, W. Shaofeng, and W. Xiaozhi, arXiv:1305.4789v2 (2013).
5. F. Benhart, J. Kotakoski, and A. V. Krashennnikov, *ASC Nano* **5**, 26 (2011).
6. G. R. Berdiyrov and F. M. Peeters, *RSC Adv.* **4**, 1133 (2014).
7. S. Li, Y. Wu, Y. Tu, et al., *Sci. Rep.* **5**, 7881 (2015).

8. B. Peng, C. Cheng, Z. Tao, and J. Chen, *J. Chem. Phys.* **133**, 034701 (2010).
9. M. H. Park, M. G. Kim, J. Joo, et al., *Nano Lett.* **9**, 3844 (2009).
10. S. H. Ng, J. Z. Wang, D. Wexler, et al., *Angew. Chem., Int. Ed.* **45**, 6896 (2006).
11. C. K. Chan, H. Peng, G. Liu, et al., *Nat. Nanotechnol.* **3**, 31 (2008).
12. G. A. Tritsarlis, E. Kaxiras, S. Meng, and E. Wang, *Nano Lett.* **13**, 2258 (2013).
13. J. Tersoff, *Phys. Rev. B* **38**, 9902 (1988).
14. J. Tersoff, *Phys. Rev. B* **39**, 5566 (1989).
15. F. Benkabou, M. Certier, and H. Aourag, *Mol. Simul.* **29**, 201 (2003).
16. R. Yu, P. Zhai, G. Li, and L. Liu, *J. Electron. Mater.* **41**, 1465 (2012).
17. S. K. Das, D. Roy, and S. Sengupta, *J. Phys. F: Metal. Phys.* **7**, 5 (1977).
18. T.-E. Fang and J.-H. Wu, *Comp. Mater. Sci.* **43**, 785 (2008).
19. K. Kawahara, T. Shirasawa, R. Arafune, et al., *Surf. Sci.* **623**, 25 (2014).
20. M. Neek-Amal, A. Sadeghi, G. R. Berdiyrov, and F. M. Peeters, *Appl. Phys. Lett.* **103**, 261904 (2013).
21. S. Plimpton, *J. Comp. Phys.* **117**, 1 (1995).

Translated by L. Mosina